Inorg. Chem. **2007**, *46*, 1789–1794

Photoinduced Spin Transition for Iron(II) Compounds with Liquid-Crystal Properties

Shinya Hayami,*,† Natsuko Motokawa,† Aya Shuto,† Naoji Masuhara,† Takehiro Someya,† Yoshihiro Ogawa,‡ Katsuya Inoue,§ and Yonezo Maeda†

Department of Chemistry, Graduate School of Science, Kyushu University, 6-10-1 Hakozaki, Higashi-ku, Fukuoka 812-8581, Japan, Department of Chemistry, Faculty of Science, Kumamoto University, 2-39-1 Kurokami, Kumamoto 860-8555, Japan, and Department of Chemistry, Faculty of Science, Hiroshima University, Higashi-Hiroshima 739-8526, Japan

Received August 31, 2006

The iron(II) compounds $[Fe(3Cn\text{-}L)_2(NCS)_2]$ ($n = 6$ (**1**), $n = 8$ (**2**), $n = 10$ (**3**), $n = 12$ (**4**), $n = 14$ (**5**), $n = 16$ (**6**), $n = 18$ (**7**), $n = 20$ (**8**), and $n = 22$ (**9**)) were synthesized and their physical properties characterized by polarizing optical microscopy, differential scanning calorimetry, and powder X-ray analysis, where 3C*n*-L denotes bidentate Schiff-base ligands formed from the corresponding aniline derivatives and pyridine-2-carboxyaldehyde. The iron(II) compounds **4**–**8** exhibited crystal to liquid-crystal transitions at 318, 334, 345, 338, and 347 K, respectively. Variable-temperature magnetic susceptibility measurements revealed that the compounds **1**–**9** exhibit spin-crossover behavior between the high-spin and low-spin states and a photoinduced spin transition from a low-spin state to a metastable high-spin state. Therefore, the iron(II) compounds **4**–**8** can undergo spin-crossover and photoinduced spin transition as well as have liquid-crystal properties all in a single molecule. Compounds with multifunctions are important in the development of molecular switches and optical materials.

Introduction

Liquid crystals are fascinating functional materials and are important in the field of advanced materials such as electrooptic devices. Organic liquid crystals are diamagnetic and can be easily oriented by an electric field. It is also possible to align liquid crystals by a magnetic field in a manner similar to that by an electric field. The construction of metal-containing liquid crystals (*metallomesogens*) has recently attracted a great deal of attention.[1−8] Strong magnetic fields are necessary for the alignment of diamagnetic liquid crystals. On the other hand, metallomesogens containing unpaired electrons are paramagnetic liquid crystals, and the magnetic field strength required to align these is much smaller than that required to align diamagnetic liquid crystals. An investigation of magnetic liquid crystals containing rare-earth ions has been reported, because these ions often have a large magnetic anisotropy.[2] Furthermore, in the development of ferromagnets with liquid-crystal properties, side-chain nickel(II) polymeric compounds have been synthesized and shown to exhibit cooperative magnetic properties.[3] Therefore, the development of metallomesogens with multifunctions (spin-crossover, mixed-valence, magnetism, conductivity, etc.) is very important to achieve the co-occurrence of various physical properties in the functional molecular-based materials.

The spin-crossover (SCO) phenomenon occurs when transforming between high-spin (HS) and low-spin (LS) states reversibly, stimulated by external perturbations (e.g., temperature, pressure, magnetic field, or light) when the

* To whom correspondence should be addressed. E-mail: hayascc@mbox.nc.kyushu-u.ac.jp. Tel: +81-92-642-2589. Fax: +81-92-642-2589.
† Kyushu University.
‡ Kumamoto University.
§ Hiroshima University.

(1) Serrano, J. L. *Metallomesogens*; VCH: Weinheim, Germany, 1996.
(2) Binnemans, K.; Galyametdinov, Y. G.; Deun, R. V.; Bruce, D. W.; Collinson, S. R.; Polishchuk, A. P.; Bikchantaev, I.; Haase, W.; Prosvirin, A. V.; Tinchurina, L.; Litvinov, I.; Gubajdullin, A.; Rakhmatullin, A.; Uytterhoeven, K.; Meervelt, L. V. *J. Am. Chem. Soc.* **2000**, *122*, 4335.
(3) Werner, R.; Falk, K.; Ostrovsky, S.; Haase, W. *Macromol. Chem. Phys.* **2001**, *202*, 2813.
(4) Piechocki, C.; Simon, J.; Skoulios, A.; Guillon, D.; Weber, P. *J. Am. Chem. Soc.* **1982**, *104*, 5245.
(5) Giround-Godquin, A. M.; Marchon, J. C. *J. Phys. Lett.* **1984**, *45*, L681.
(6) Galyametdinov, Y.; Ksenofontov, V.; Prosvirin, A.; Ovchinnikov, I.; Ivanova, G.; Gütlich, P.; Haase, W. *Angew. Chem., Int. Ed.* **2001**, *40*, 4269.
(7) Real, J. A.; Gasper, A. B.; Niel, V.; Muñoz, M. C. *Coord. Chem. Rev.* **2003**, *236*, 121.
(8) Real, J. A.; Gasper, A. B.; Muñoz, M. C. *Dalton Trans.* **2005**, 2062.

10.1021/ic061646g CCC: $37.00
Published on Web 02/02/2007

ligand field strength is comparable to the mean spin-pairing energy. At low temperature, the thermodynamically stable state is the LS state, of lowest enthalpy.[9] On the other hand, when the temperature is higher than SCO temperature, denoted $T_{1/2}$, the HS state becomes the thermodynamically stable state, because the entropy associated with the HS state is much greater than that associated with the LS state. It may be possible that both the SCO and crystal to liquid-crystal transition can be synchronized in a single molecule: (i) the SCO compounds with $T_{1/2}$ above room temperature are necessary because the crystal to liquid-crystal transition temperature is generally higher than room temperature for the metallomesogens, or (ii) the crystal to liquid-crystal transition temperature can be adjusted to $T_{1/2}$ of the SCO compounds by changing the length and type of the alkyl chains. Furthermore, it would be interesting to investigate the dielectric and ferroelectric properties from the point of view of the application of these materials in future molecular devices.

The fascinating peculiarities of SCO compounds stimulated the idea of combining liquid crystalline and SCO behavior in a single molecule. Galyametdinov and co-workers reported such a SCO iron(III) compound ($S = {}^1/_2 \leftrightarrow S = {}^5/_2$) with liquid-crystal properties.[6] This compound consists of an iron(III) ion coordinated to Schiff-base ligands with long alkyl chains and exhibits a rodlike geometry. The SCO behavior was gradual in the temperature range of 4.2−293 K, and the smectic A mesophase was observed between 380 and 418 K. Fujigaya et al. have reported a one-dimensional iron(II) compound with triazole derivatives, which exhibits SCO and liquid-crystal behavior in the same temperature region.[10,11] However, the supposed mesomorphism of the complexes has not been confirmed. Gaspar et al. have been investigating the possibility of synchronizing both transitions in the iron(II) complexes of $[Fe(Cn\text{-trz})_3](p\text{-tol})_2$ (n = 8, 10, and 12). They have reported that the complexes exhibit a transition from the crystalline state to the mesophase state, which takes place synchronously with the spin transition.[12,24]

For iron(II) SCO compounds ($S = 0 \leftrightarrow S = 2$), light-induced LS → HS conversion can be observed by illumination. A mechanism for this phenomenon, denoted as "light-induced excited spin-state trapping" (LIESST), has been proposed.[13,14] The development of novel compounds exhibiting LIESST is one of the main challenges in this field.[13−17]

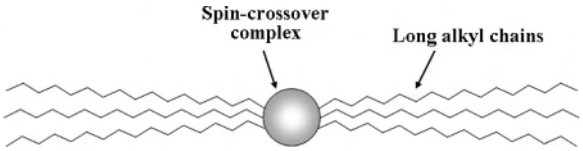

Figure 1. Construction of the *metallomesogen* with spin-crossover phenomenon.

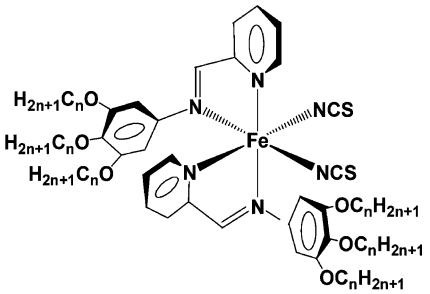

Figure 2. Chemical structure of the *metallomesogen* with a spin-crossover core, $[Fe(3Cn\text{-L})_2(NCS)_2]$.

The LIESST compounds can be used as optical switching molecular devices, and various functional materials including optical switches can be constructed.

Here, we focused on the SCO iron(II) compounds in order to control the liquid crystals, not only by temperature but also by photoillumination.[18,19] The design of metallomesogens containing an SCO iron(II) center has stimulated the production of unexpected advanced materials by combining SCO, LIESST, and liquid-crystal properties (Figure 1).[20] The iron(II) compounds $[Fe(3Cn\text{-L})_2(NCS)_2]$ (n = 6 (**1**), 8 (**2**), 10 (**3**), 12 (**4**), 14 (**5**), 16 (**6**), 18 (**7**), 20 (**8**), and 22 (**9**)) were designed in order to construct a SCO material with liquid-crystal properties (Figure 2), where 3Cn-L are Schiff-base bidentate ligands derived from the condensation of aniline derivatives (with three long alkyl chains) and pyridine-2-carboxyaldehyde (Scheme 1).

Results and Discussion

The iron(II) compounds $[Fe(3Cn\text{-L})_2(NCS)_2]$ were synthesized on the basis of the structure of $[Fe(PM\text{-A})_2(NCS)_2]$ (PM = pyridylmethylene, A = aniline), in which the PM-A ligand comprises long alkyl chains (n is the length of the methylene chain, n = 6 (**1**), 8 (**2**), 10 (**3**), 12 (**4**), 14 (**5**), 16 (**6**), 18 (**7**), 20 (**8**), and 22 (**9**)).[20] For compounds **1**−**9**, it was not possible to prepare single crystals; therefore, the geometrical optimization of these complexes was performed by computer simulation.[21] Létard et al. reported that the iron atom was surrounded by six nitrogen atoms belonging to the two NCS^- groups in cis positions and two bidentate

(9) Kahn, O. *Molecular Magnetism*; VCH: New York, 1993.
(10) Fujigaya, T.; Jiang, D.-L.; Aida, T. *J. Am. Chem. Soc.* **2003**, *125*, 14690.
(11) Fujigaya, T.; Jiang, D.-L.; Aida, T. *J. Am. Chem. Soc.* **2005**, *127*, 5484.
(12) Gaspar, A. B.; Ksenofontov, V.; Seredyuk, M.; Gütlich, P. *Coord. Chem. Rev.* **2005**, *249*, 2661.
(13) Decurtins, S.; Gütlich, P.; Köhler, C. P.; Spiering, H.; Hauser, A. *Chem. Phys. Lett.* **1984**, *105*, 1.
(14) Gütlich, P.; Hauser, A.; Spiering, H. *Angew. Chem., Int. Ed. Engl.* **1994**, *33*, 2024.
(15) Létard, J.-F.; Guionneau, P.; Nguyen, O.; Costa, J. S.; Marcen, S.; Chastanet, G.; Marchivie, M.; Goux-Capes, L. *Chem.—Eur. J.* **2005**, *11*, 4582.
(16) *Spin Crossover in Transition Metal Compounds;* Topics in Current Chemistry; Gütlich, P., Goodwin. H. A., Eds.; Springer-Verlag: Berlin, Heidelberg, New York, 2004; Vols. 233−235.
(17) Hayami, S.; Gu, Z.-Z.; Shiro, M.; Einaga, Y.; Fujishima, A.; Sato, O. *J. Am. Chem. Soc.* **2000**, *122*, 11569−11570.
(18) Hayami, S.; Danjobara, K.; Inoue, K.; Ogawa, Y.; Matsumoto, N.; Maeda, Y. *Adv. Mater. (Weinheim, Ger.)* **2004**, *16*, 869.
(19) Hayami, S.; Danjobara, K.; Miyazaki, S.; Inoue, K.; Ogawa, Y.; Maeda, Y. *Polyhedron* **2005**, *24*, 2821.
(20) Ksenofontov, V.; Levchenko, G.; Spiering, H.; Gütlich, P.; Létard, J.-F.; Bouhedja, Y.; Kahn, O. *Chem. Phys. Lett.* **1998**, *294*, 545.
(21) A geometry optimization for the compounds was performed in the gas phase by using Chem3D Ultra 10.0.

Scheme 1. Synthesis of the Ligand 3C*n*-L[a]

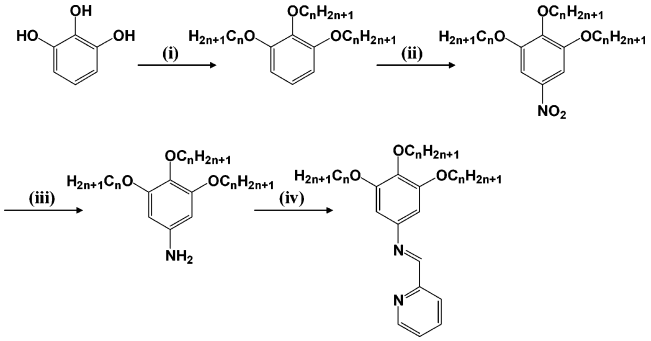

[a] Reagents and conditions: (i) $C_nH_{2n+1}Br$, K_2CO_3, 80 °C, 6 h; (ii) HNO_3, SiO_2, 1 h; (iii) hydrazine, Pd−C, 24 h; (iv) pyridine-2-carboxyaldehyde, 3 h.

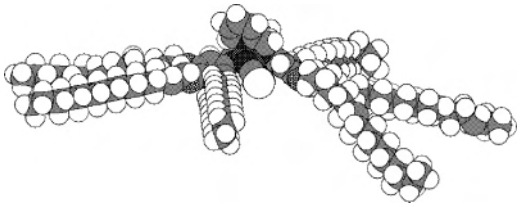

Figure 3. Computer simulation of the molecular structure of compound **6**.

ligands.[22,23] Since the iron(II) compound *cis*-bis(thiocyanato)-bis[*N*-(2-pyridylmethylene)aniline]iron(II) exhibits SCO and the LIESST effect, the PM-A ligand was modified to give a Schiff-base ligand with elongated substituents (Figure 2). In consideration of the structure of the SCO iron(II) compounds, the structures of compounds **1**−**9** have been optimized. The resultant geometrical structure of **6** is shown in Figure 3. A twisted-structure or starfish-like geometry has been proposed for the molecular structures of compounds **1**−**9**.

Phase transition enthalpy changes were measured by carrying out differential scanning calorimetry (DSC) thermal analysis for compounds **1**−**9**. The DSC curves of **1**−**9** are shown in parts a and b of Figure 4 . One endothermic peak was observed during the heating mode of compounds **1**, **2**, **3**, and **9**, which has been assigned to the corresponding melting points of these materials. It has been revealed that compounds **1**, **2**, **3,** and **9** with alkyl chain lengths of $n = 6$, 8, 10, and 22 do not exhibit crystal-mesophase transitions. On the other hand, two peaks were observed in the DSC spectra for compounds **4**−**8**. For compound **4**, the first peak at 318 K ($\Delta H = 29.4$ kJ mol^{-1}) was assigned to a crystal-mesophase transition and that at 404 K ($\Delta H = 16.0$ kJ mol^{-1}) was assigned to a mesophase-liquid transition. For compound **5**, the first peak at 333 K ($\Delta H = 82.2$ kJ mol^{-1}) was assigned to a crystal-mesophase transition, and the second peak at 402 K ($\Delta H = 26.3$ kJ mol^{-1}) was assigned to a mesophase-liquid transition. For compound **6**, the first peak at 342 K ($\Delta H = 142.3$ kJ mol^{-1}) was assigned to a crystal-mesophase transition, and the peak at 399 K ($\Delta H = 24.1$ kJ mol^{-1}) was assigned to a mesophase-liquid transition. For compound **7**, the first peak at 338 K ($\Delta H = 146.2$ kJ mol^{-1}) was assigned to a crystal-mesophase transition, and the peak at 389 K ($\Delta H = 17.0$ kJ mol^{-1}) was assigned to a mesophase-liquid transition. For compound **8**, the first peak at 347 K ($\Delta H = 198.2$ kJ mol^{-1}) was assigned to a crystal-mesophase transition, and the peak at 392 K ($\Delta H = 21.4$ kJ mol^{-1}) was assigned to a mesophase-liquid transition. The large peak observed at low temperature was assigned to the crystal-mesophase transition, whereas the smaller peak at high temperature was assigned to the mesophase-liquid transition. The temperatures of the crystal-mesophase and mesophase-liquid transitions for compounds **1**−**9** are summarized in Table 1. The DCS results were measured in the temperature range corresponding to the transition from the crystal to liquid-crystal state on warming and cooling reversibly. On cooling, the transition temperatures for the mesophase-crystal transition of compounds **4**−**8** were observed at 299, 310, 325, 335, and 340 K, respectively. The free ligands, **3C*n*-L** ($n = 6-22$), exhibit only one peak, assigned to the melting point of the ligand.

The mesophase was studied by hot-stage polarized optical microscopy, and the texture of the liquid-crystal state was observed by optical microscopy. Compounds **4**−**8** were observed in the solid state at room temperature. The compounds were heated on the stage of the optical microscope under polarized light and shown to exhibit mesomorphism. On heating, the compounds underwent a transition from the solid state to a birefringent viscous fluid and exhibited a characteristic mosaic texture. When the compounds were cooled from the isotropic liquid state to room temperature, the same mosaic texture was observed as that seen prior to heating. An example of this texture is revealed for **8** observed under crossed polarizers, as shown in Figure 5. The same texture of **8** was also observed for compounds **4**−**7**. The phase of the liquid-crystal state has not been identified on the basis of the texture observed by optical microscopy.

Temperature-dependent X-ray diffraction (XRD) measurements were carried out to confirm the existence of this mesophase. Figure 6a shows the powder XRD patterns of the crystal and mesophase states for compound **4**, observed in the temperature range from 290 to 330 K. A sharp reflection in the low-angle area ($2\theta = 4.1°$) with *d*-spacing of 21.5 Å was detected at 290 and 310 K. This *d*-spacing may correspond to the length of the elongated substituents. At 330 K, the peak of $2\theta = 4.1°$ disappeared and a new peak appeared at $2\theta = 2.6°$ ($d = 33.9$ Å). The peak of $2\theta = 19.5°$ ($d = 4.6$ Å) observed below 310 K broadened simultaneously. The formation of the mesophase is completed in the temperature range between 310 and 330 K, in accordance with the result observed in DSC. The powder patterns for compounds **5** and **6** also changed in the low-angle region, from $2\theta = 3.8°$ ($d = 23.2$ Å) to $2\theta = 2.3°$ ($d = 38.4$ Å) for **5** (Figure 6b) and from $2\theta = 3.4°$ ($d = 26.0$ Å) to $2\theta = 2.2°$ ($d = 40.1$ Å) for **6** (Figure 6c). On the other hand, the changes in the powder XRD patterns for **7**

(22) Létard, J.-F.; Guionneau, P.; Codjovi, E.; Lavastre, O.; Bravic, G.; Chasseau, D.; Kahn, O. *J. Am. Chem. Soc.* **1997**, *119*, 10861.
(23) Létard, J.-F.; Guionneau, P.; Rabardel, L.; Howard, J. A. K.; Goeta, A. E.; Chasseau, D.; Kahn, O. *Inorg. Chem.* **1998**, *37*, 4432.
(24) Seredyuk, M.; Gaspar, A. B.; Ksenofontov, V.; Reiman, S.; Galyametdinov, Y.; Haase, W.; Rentschler, E.; Gütlich, P. *Chem. Mater.* **2006**, *18*, 2513.

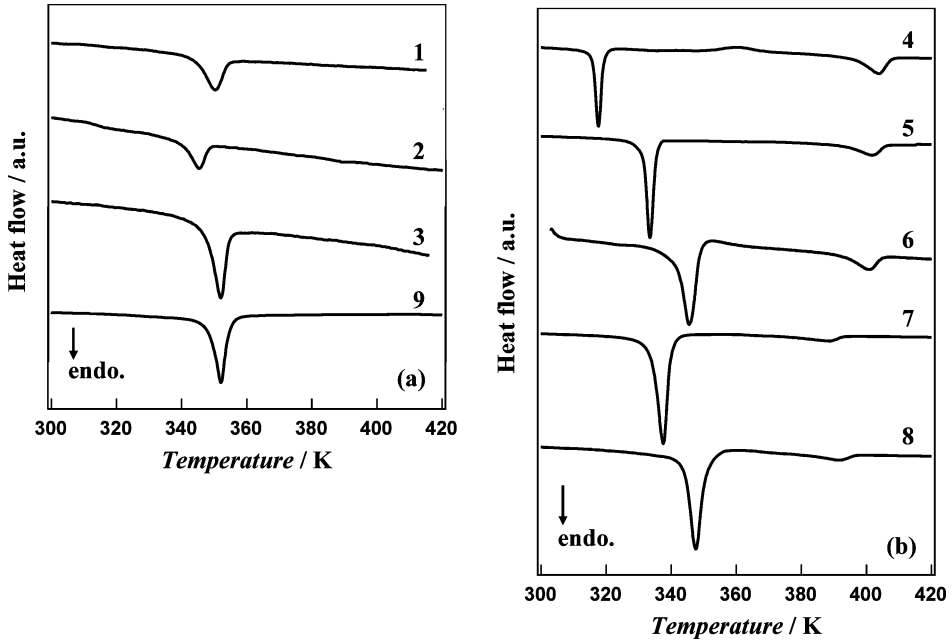

Figure 4. DSC of compounds **1**−**3** and **9** (a) and **4**−**8** (b).

Table 1. Phase Transition Temperatures for **1**−**9**[a]

	transition temperature/K			
compound	Cr-LQ	LQ-L	SCO	*T*(LIESST)
1, $n = 6$		350	173	63
2, $n = 8$		345	159	61
3, $n = 10$		352	129	65
4, $n = 12$	318	404	230	61
5, $n = 14$	333	402	223	55
6, $n = 16$	342	399	221	61
7, $n = 18$	338	389	214	57
8, $n = 20$	347	392	205	59
9, $n = 22$		352	177	61

[a] Cr is solid state, LQ is liquid-crystal state, and L is liquid state.

Figure 5. Texture of compound **8** under crossed polarizers at 380 K.

and **8** were different from those for **4**−**6**. Figure 6d show the powder XRD patterns of the crystal and mesophase states for compound **7**, observed in the temperature range from 290 to 350 K. A reflection in the low-angle region was not observed at 290 or 310 K, because the reflection peak is in a lower angle area than $2\theta = 2.0°$. After the liquid-crystal transition at 350 K, a new peak appeared at $2\theta = 2.3°$ ($d =$ 37.8 Å), and the peak of $2\theta = 21.6°$ ($d = 4.1$ Å) observed below 310 K was found to broaden. The formation of the mesophase is completed in the temperature range between 310 and 350 K, in accordance with the results observed in the DSC study. The powder XRD patterns for compound **8** also changed, in accordance with those for **7**, from $2\theta <$ 2.0° ($d >$ 44.1 Å) to $2\theta = 2.2°$ ($d = 40.1$ Å) for **8** (Figure 6e). After the liquid-crystal transition, the *d*-spacing was found to increase for compounds **4**−**6** and decrease for **7**−**8**. It is thought that the phase transition behaviors are different between compounds **4**−**6** and **7**−**8**.

The SCO phenomenon observed between the HS and LS states for compounds **1**−**9** was followed by measurements of the molar magnetic susceptibility χ_m as a function of temperature. The product $\chi_m T$ for the SCO material is determined by the temperature-dependent contributions χ_{mHS} and χ_{mLS} according to $\chi_m(T) = \gamma_{HS}\chi_{mHS} + (1 - \gamma_{HS})\chi_{mLS}$. The $\chi_m T$ vs T plots for compounds **1**−**9** are given in Figure 7. Compounds **1**−**3** and **9** do not exhibit a mesophase transition. The $\chi_m T$ value for compound **1** is equal to 1.75 cm^3 K mol^{-1} below 70 K, which shows that about 62% of the iron(II) ions remained in the HS state. It is thought that the decrease of the $\chi_m T$ value below 30 K is due to zero-field splitting. On heating, the $\chi_m T$ values were almost constant from 30 to 70 K and gradually increased around the spin transition temperature, $T_{1/2} = 173$ K (Table 1). The $\chi_m T$ value at 320 K was ca. 2.82 cm^3 K mol^{-1}, and an incomplete gradual SCO phenomenon was observed. A jump in the $\chi_m T$ value was observed at 367 K, which is in accordance with the melting point in the DSC data. This increase may be explained as a molecular reorientation due to melting. When the samples of compound **1** were il-

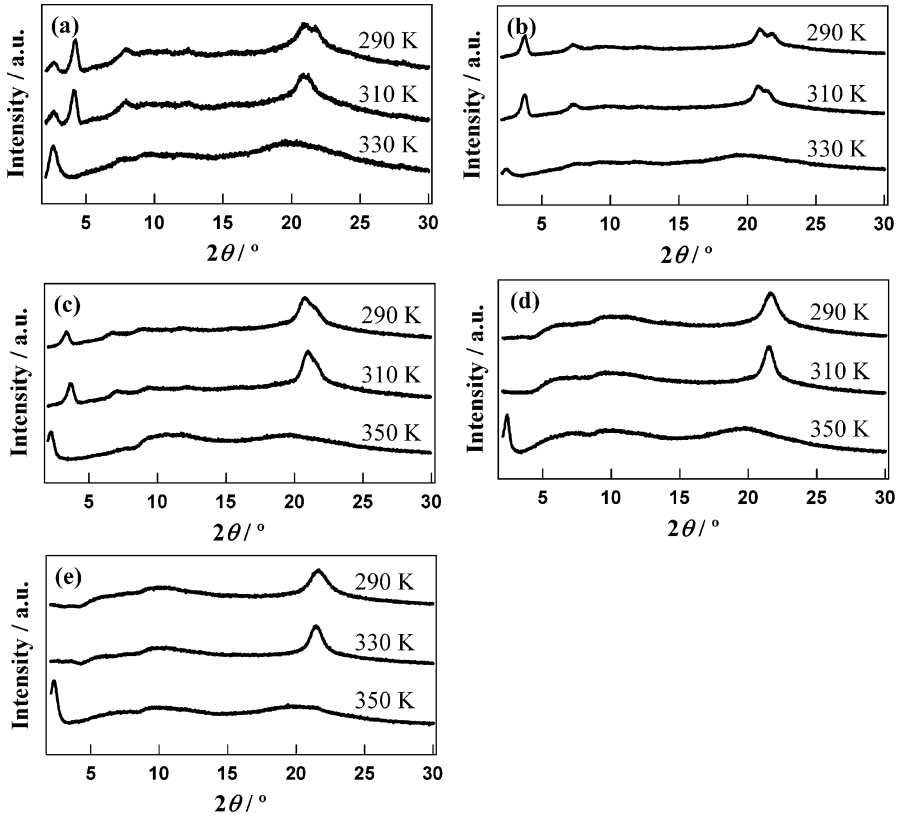

Figure 6. Temperature dependence of the powder XRD pattern for compounds **4** (a), **5** (b), **6** (c), **7**(d), and **8** (e).

luminated (at 532 nm) at 5 K for 1 h, the $\chi_m T$ value increased. This change in the $\chi_m T$ value persisted for many hours, even after the illumination was stopped. This suggests that the transition from the LS to HS state can be partially induced by illumination. The relaxation temperature of the LIESST effect is defined as T(LIESST), and the temperature dependence of $\chi_m T$ after illumination shows that the $\chi_m T$ value decreases with increasing temperature and that thermal relaxation to the ground state occurs. The T(LIESST) is 63 K, and compound **1** was found to exhibit photoswitching below this temperature (Table 1). About 51% of the LS fraction was induced by illumination. The SCO and LIESST behaviors for compounds **2**, **3**, and **9** were also similar to that of **1**. The observed spin transition temperatures were $T_{1/2} = 159$ K for **2**, $T_{1/2} = 129$ K for **3,** and $T_{1/2} = 177$ K for **9**. The T(LIESST) is 61 K for **2**, 65 K for **3**, and 61 K for **9**. It was found that the longer the alkyl chains lengths, the lower the spin transition temperatures for **1**−**3**. The T(LIESST) was almost constant for compounds **1**−**3** and **9**.

On the other hand, the magnetic behaviors for compounds **4**−**8** exhibiting liquid-crystal transitions were different from those for compounds **1**−**3** and **9**. The $\chi_m T$ value for compound **4** is equal to 0.55 cm^3 K mol^{-1} below 80 K, which shows that about 17% of the iron(II) ions remained in the HS state. On heating, the $\chi_m T$ values were almost constant from 5 to 80 K and gradually increased at around the spin transition temperature, $T_{1/2} = 230$ K. The $\chi_m T$ value at 360 K was ca. 3.25 cm^3 K mol^{-1}, showing that the SCO from the LS to HS state is induced. The $\chi_m T$ jump associated with the crystal to liquid-crystal transition was observed at 321 K and indicates that the crystal to liquid-crystal transition may be caused by alignment of the liquid-crystal molecules. Compound **4** also exhibited a LIESST effect, with a T(LIESST) value of 61 K, where about 46% of the LS fraction was induced to the HS state by illumination. The SCO and LIESST behaviors for compounds **5**−**7** were also similar to that of **4**. The spin transition temperatures were $T_{1/2} = 223$ K for **5**, $T_{1/2} = 221$ K for **6**, $T_{1/2} = 214$ K for **7**, and $T_{1/2} = 205$ K for **8**. The T(LIESST) is 55 K for **5**, 61 K for **6**, 57 K for **7**, and 59 K for **8**. It was determined that the longer the alkyl chains lengths, the greater the decrease in spin transition temperature for compounds **4**−**8**. The T(LIESST) value was almost constant for **4**−**8**.

The SCO temperatures $T_{1/2}$ for compounds **1**−**3** and **9** (which do not exhibit mesophase transitions) occur in the temperature range of 129−177 K, where the observed temperatures are lower than those for compounds **4**−**8** (205−230 K), which exhibit mesophase transitions. The fractions of the SCO from the HS to LS state were 38%, 41%, 41%, and 35% for compounds **1**−**3** and **9** (which do not exhibit mesophase transitions), respectively. On the other hand, the fractions were 83%, 86%, 82%, 69%, and 55% for compounds **4**−**8**, which all exhibit mesophase transitions, respectively. The SCO fractions for compounds **4**−**8** were larger than those for compounds **1**−**3** and **9**. Furthermore, the SCO fractions for **4**−**6** were between 82 and 86%, whereas the fractions for **7**−**8** were between 51 and 65%. The differences in the SCO fractions may be caused by the differences in the mesophase transition behaviors; the *d*-spacing was observed to increase for compounds **4**−**6** and

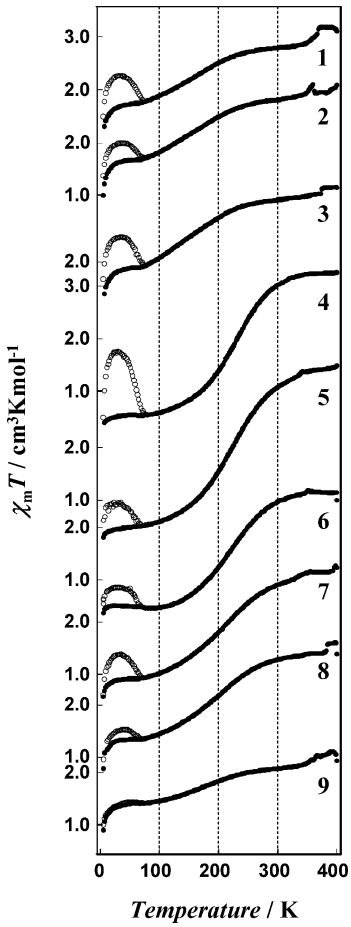

Figure 7. $\chi_m T$ versus T plots (●) for compounds **1**−**9**. $\chi_m T$ versus T plots for the LIESST experiment were recorded in the warming mode (○).

decrease for compounds **7** and **8** after the mesophase transition.

Conclusion

Iron(II) compounds (**1**−**9**) with long alkyl chains have been synthesized, and their properties have been characterized. Compounds **4**−**8** exhibited liquid-crystal properties, as confirmed from the results of DSC and XRD diffractions and the texture of the compounds observed under crossed polarizers. Compounds **1**−**9** exhibited SCO phenomena. Furthermore, compounds **1**−**9** exhibited the LIESST effect; i.e., three physical properties, spin-crossover, the LIESST effect, and liquid-crystal properties, can coexist in a single molecule for compounds **4**−**8**. Moreover, the behaviors of the mesophase transitions for compounds **4**−**6** were different from those for compounds **7**−**8**; the *d*-spacing for compounds **4**−**6** increases, whereas the *d*-spacing for **7**−**8** decreases after the mesophase transition. Geometrical flexibility in the molecules is very important in order to achieve co-occurrence of various physical properties in the functional molecular-based materials. We believe that our approach, i.e., the co-occurrence of SCO, LIESST, and liquid-crystal properties, can be widely applied, not only in the design of LIESST compounds with liquid-crystal properties but also in the design of a variety of optically switchable molecular compounds.

Experimental Section

Instruments. ^{1}H NMR was measured on a Bruker AVANCE SERIES DPX 400 instrument operating at 400 MHz (using the deuterated solvent as the lock and the residual solvent or tetramethylsilane as the internal reference). Magnetic susceptibilities of the ground samples were measured on a Quantum Design MPMS-5S. Samples were placed into a gelatin capsule, mounted inside a full length straw, and then fixed to the end of the sample transport rod. Illumination experiments were performed using a Nd:YVO_4 laser ($\lambda = 532$ nm) as a light source. The light was guided via an optical fiber into the SQUID magnetometer. The sample was placed on the edge of the optical fiber. The Mössbauer spectra (isomer shift vs metallic iron at room temperature) were measured using a Wissel MVT-1000 Mössbauer spectrometer with a ^{57}Co/Rh source in the transmission mode. All isomer shifts are given relative to α-Fe at room temperature. The measurements at low temperature were performed with a closed-cycle helium refrigerator cryostat (Iwatani Co., Ltd.). DSC thermal analysis was carried out on a SHIMADZU DSC50 differential scanning calorimeter. XRD studies were performed on a Rigaku X-ray diffractometer RAD-2A with a 2.0 kW Cu Kα X-ray. Optical polarized microscopy was carried out on a Nippon Chemical Industrial Corporation polarization microscope (OPTICAL POL with a Yanagimoto factory model MP-J3) micromelting point meter.

Materials. Unless otherwise noted, all starting materials were purchased from commercial sources and were used as obtained. All the ligands (**3C*n*-L**, $n = 6-22$) and iron(II) compounds [Fe(3C*n*-L)$_2$(NCS)$_2$] (**1**−**9**) were synthesized according to the method described previously.[18,19] Anal. Calcd for $C_{62}H_{92}N_6O_6S_2$ (**1**): C, 65.47; H, 8.15; N, 7.39. Found: C, 65.25; H, 8.08; N, 7.29. Anal. Calcd for $C_{74}H_{116}N_6O_6S_2$ (**2**): C, 68.48; H, 8.99; N, 6.14. Found: C, 68.37; H, 8.95; N, 6.34. Anal. Calcd for $C_{86}H_{140}N_6O_6S_2$ (**3**): C, 69.89; H, 9.50; N, 5.67. Found: C, 70.07; H, 9.57; N, 5.70. Anal. Calcd for $C_{98}H_{164}N_6O_6S_2$ (**4**): C, 70.83; H, 9.87; N, 5.04. Found: C, 70.67; H, 10.06; N, 5.12. Anal. Calcd for $C_{110}H_{188}N_6O_6S_2$ (**5**): C, 71.85; H, 10.31; N, 4.54. Found: C, 71.97; H, 10.47; N, 4.64. Anal. Calcd for $C_{122}H_{212}N_6O_6S_2$ (**6**): C, 74.04; H, 10.80; N, 4.25. Found: C, 73.71; H, 10.71; N, 4.19. Anal. Calcd for $C_{134}H_{236}N_6O_6S_2$ (**7**): C, 75.25; H, 11.11; N, 3.75. Found: C, 75.05; H, 11.08; N, 3.91. Anal. Calcd for $C_{146}H_{260}N_6O_6S_2$ (**8**): C, 76.40; H, 11.52; N, 3.38. Found: C, 76.60; H, 11.70; N, 3.09. Anal. Calcd for $C_{158}H_{284}N_6O_6S_2$ (**9**): C, 75.73; H, 11.32; N, 3.63. Found: C, 75.90; H, 11.38; N, 3.35.

Acknowledgment. This work was supported by a Grant-in-Aid for Scientific Research (No. 17750130) from the Ministry of Education, Culture, Sports, Science and Technology of the Japanese Government, the Inamori Foundation, the Kato Foundation, and "Development of Molecular Devices in Ferroelectric Metallomesogens" in 2006 from the New Energy and Industrial Technology Development Organization (NEDO) of Japan.

IC061646G